Semiquantitative Approach to Amyloid Positron Emission Tomography Interpretation in Clinical Practice

Ana M. Franceschi[1]   David R. Petrover[1]   Luca Giliberto[2,3]   Sean A. P. Clouston[4]   Marc L. Gordon[3,5]

[1] Neuroradiology Section, Department of Radiology, Lenox Hill Hospital, Donald and Barbara Zucker School of Medicine at Hofstra/Northwell, New York, New York, United States
[2] Institute for Neurology and Neurosurgery, Donald and Barbara Zucker School of Medicine at Hofstra/Northwell, Manhasset, New York, United States
[3] Litwin-Zucker Research Center, Feinstein Institutes for Medical Research, Northwell Health, New York, United States
[4] Department of Family, Population and Preventative Medicine and Program in Public Health, Renaissance School of Medicine at Stony Brook University, Stony Brook, New York, United States

Address for correspondence Ana M. Franceschi, MD, PhD, Department of Radiology, Lenox Hill Hospital, 100 East 77th Street, 3rd Floor, New York, NY, 10075, United States (e-mail: afranceschi@northwell.edu).

[5] Departments of Neurology and Psychiatry, Donald and Barbara Zucker School of Medicine at Hofstra/Northwell, New York, United States

Abstract

Objective   Amyloid positron emission tomography (PET) plays a vital role in the in vivo detection of β-amyloid accumulation in Alzheimer's disease. Increasingly, trainees and infrequent readers are relying on semiquantitative analyses to support clinical diagnostic efforts. Our objective was to determine if the visual assessment of amyloid PET may be facilitated by relying on semiquantitative analysis.

Methods   We conducted a retrospective review of [18F]-florbetaben PET/computed tomographies (CTs) from 2016 to 2018. Visual interpretation to determine Aβ+ status was conducted by two readers blinded to each other's interpretation. Scans were then post-processed utilizing the MIMneuro software, which generated regional-based semiquantitative Z-scores indicating cortical Aβ-burden.

Results   Of 167 [18F]-florbetaben PET/CTs, 92/167 (reader-1) and 101/167 (reader-2) were positive for amyloid deposition (agreement $=92.2\%$, $\kappa = 0.84$). Additional nine scans were identified as possible Aβ-positive based solely on semiquantitative analyses. Largest semiquantitative differences were identified in the left frontal lobe ($Z = 7.74$ in Aβ$+$; 0.50 in Aβ$-$). All unilateral regions showed large statistically significant differences in Aβ-burden ($P \le 2.08E-28$). Semiquantitative scores were highly sensitive to Aβ+ status and accurate in their ability to identify amyloid positivity, defined as a positive scan by both readers (AUC ≥ 0.90 [0.79–1.00]). Spread analyses suggested that amyloid deposition was most severe in the left posterior cingulate gyrus. The largest differences between Aβ$+$/Aβ$-$ were in the left frontal lobe. Analyses using

Keywords
► β-amyloid
► 18F-florbetaben
► PET/CT
► brain PET
► Alzheimer's disease

region-specific cutoffs indicated that the presence of amyloid in the temporal and anterior cingulate cortex, while exhibiting relatively low Z-scores, was most common. **Conclusion**   Visual assessment and semiquantitative analysis provide highly congruent results, thereby enhancing reader confidence and improving scan interpretation. This is particularly relevant, given recent advances in amyloid-targeting disease-modifying therapeutics.

Introduction

The most common cause of neurodegenerative dementia is Alzheimer's disease (AD), accounting for 60–80% of all dementias and affecting over 6 million people in the USA and 50 million people worldwide. AD is a leading cause of mortality in the elderly (sixth-leading cause of death in the United States and the fifth-leading cause of death among Americans aged 65 years and older) and, with increasing longevity, is projected to impact up to 13.8 million people in the USA by 2060 with an associated significant rise in healthcare cost, which is projected to exceed $1 trillion by 2050.[1–3] Histopathologically, the AD cascade, originally described by Alois Alzheimer in 1907, is characterized by brain infiltration of two amyloid-β (Aβ) isoforms ($A\beta_{1-42}$ and $A\beta_{1-40}$), leading to Aβ deposition and the formation of diffuse and dense-core Aβ plaques with concomitant phosphorylation of tau protein and accumulation of neurofibrillary tangles and neurodegeneration.[4–6] Amyloid-β in the human brain follows a distinct sequence in which the regions are hierarchically involved, beginning in the neocortex and spreading anterogradely into regions that receive neuronal projections from regions already exhibiting cortical Aβ burden, as described by Thal et al in 2002.[7] Of note, amyloid deposition precedes cognitive changes and tau deposition although the relationship between amyloid, tau, and clinical progression is complex and still needs to be fully elucidated.[8,9]

There is intense interest in minimally invasive neuroimaging biomarkers in neurodegenerative disease definitions and for use in clinical trials, particularly in the setting of novel disease-modifying therapies, where accurate confirmation of AD pathology is paramount.[10] In 2016, Jack et al outlined a novel system as an unbiased descriptive classification scheme for research purposes when characterizing patients presenting with cognitive impairment,[11,12] classifying key biomarkers into three binary categories: "A" refers to the value of total β-amyloid biomarker (amyloid positron emission tomography [PET], or cerebrospinal fluid [CSF] Aβ42 can be used); "T," to the value of a tau biomarker (tau PET, CSF p-tau, or recently plasma p-tau); and "N," to a biomarker of neurodegeneration or neuronal injury (^{18}F-fluorodeoxyglucose–PET, structural magnetic resonance imaging [MRI], CSF total tau, or plasma neurofilament light chain). Each biomarker category is rated as positive or negative and staging can be accomplished for research purposes by the presence/absence of these biomarkers. Given its independent approach to categorizing multidomain biomarker findings at the individual level, without specifying disease labels per se, it is ideally suited as a

research framework given the lack of consensus on terminology across the spectrum of cognitive aging and impairment. In fact, the A/T/N classification has been endorsed by the National Institute on Aging and the Alzheimer's Association (NIA-AA) for implementation in the research and clinical trial setting.[12,13]

In the characterization of AD for research, amyloid PET plays a vital role in in vivo detection of β-amyloid (Aβ) accumulation in patients presenting with cognitive impairment, and this is taking on a new dimension with the recent Federal Drug Administration's (FDA) approval of the first potentially disease-modifying therapy in the treatment of AD,[14] the amyloid-targeting monoclonal antibody aducanumab (trade name: Aduhelm) in June 2021. Given the first-of-its-kind treatment for AD, trainees and infrequent neuroradiological readers will be required to interpret these studies in a clinical setting, and their interpretations will have a direct impact on patient management. Therefore, semiquantitative tools available in routine clinical practice are becoming increasingly important to support diagnostic efforts. However, there are limited data assessing the correspondence between visual assessment and semiquantitative analysis in the evaluation of cortical amyloid burden.[15–17] In this study, we retrospectively reviewed ^{18}F-florbetaben PET/CT studies acquired at our institution as part of the Imaging Dementia-Evidence for Amyloid Scanning (IDEAS) study[18] to determine if the qualitative assessment of amyloid PET scans may be facilitated by relying on results from the semiquantitative analysis.

Methods

Ethics: This study received local institutional review board (IRB) approval. The IRB waived the need for written informed consent, given the retrospective nature of the study.

Patient Selection

Subjects were referred from memory clinics for ^{18}F-florbetaben PET/CT as part of the IDEAS study from June 2016 to May 2018. Eligible patients were Medicare beneficiaries age 65 years or older, English or Spanish speaking, with a diagnosis of mild cognitive impairment (MCI) or dementia established by a dementia specialist within the past 24 months. All subjects were required to have completed a comprehensive diagnostic assessment, including global cognition assessed via the Mini-Mental State Examination (range, 0 [worst] to 30 [best]) or Montreal Cognitive Assessment (range, 0 [worst] to 30 [best]) at the time of enrollment, laboratory testing within the past 12 months, and head CT or

MRI within the past 24 months. Patients were further required to meet appropriate use criteria for amyloid PET[19]: (1) the etiologic cause of cognitive impairment remained uncertain after a comprehensive evaluation by a dementia specialist, (2) Alzheimer's disease was a diagnostic consideration, and (3) knowledge of amyloid PET status was expected to alter diagnosis and management. Patients were excluded if amyloid status was already known based on prior PET or CSF analysis or if learning amyloid status could, in the opinion of the specialist, cause significant psychological harm.

Image Acquisition

Amyloid PET was completed within 30 days of the pre-PET assessment following published practice guidelines.[20] Subjects received 300 MBq (8.1 mCi) of ^{18}F-florbetabem intravenously and were placed in a quiet room during the tracer uptake period. Approximately 90 to 120 min after radiopharmaceutical injection, patients were scanned on a GE Discovery 710 PET/CT scanner. Transmission data (head CT) was acquired for approximately 2 min and parameters were as follows: kVp 120; mA 95; helical scanning; rotation = 0.8 mm/rot; and pitch = 1.375:1. Emission data (brain PET) was acquired for approximately 20 min (static acquisition with dynamic replay in 10 frames at 2 min/frame). Images were reconstructed using the VUE Point FX reconstruction with 32 subsets and two iterations; z-axis filter = "heavy" and 4.0 mm FWHM Gaussian post-filtering. Quantitative corrections included attenuation, scatter, random, detector efficiency, decay, and deadtime. Acquired PET data were scaled to injected dose and body weight to produce standardized uptake value (SUV) images.

Image Analysis

Visual interpretation to determine Aβ+ status was conducted by two independent readers blinded to each other's interpretation. One of the readers (DP) was a trainee with 1 year of experience, the other (AMF) was a board-certified neuroradiologist with dedicated PET/MRI training and 5 years of clinical and research expertise in brain PET. Studies were classified as either positive (1) or negative (0) for increased cortical Aβ burden. After qualitative reads were completed, scans were post-processed utilizing MIM-Neuro version 7.1.6 (MIM Software, Inc., Cleveland, Ohio, United States). MIMNeuro is a commercially available program that aids in the analysis and post-processing of PET and single-photon emission computed tomography (SPECT) studies. It performs voxel- and region-based comparison of radiotracer uptake between its database of normal studies and a given study with the aid of built-in anatomic atlases. The differences in radiotracer uptake are represented with a Z-score of standard deviation from normal, or the SUV ratio. For our study, MIMNeuro generated regional-based semiquantitative Z-scores, indicating cortical amyloid burden following industry standards including using the whole cerebellum as the reference region. Z-score values were reported for 12 brain regions total: right and left posterior cingulate gyrus, right and left precuneus, right and left inferior medial frontal gyrus, right and left anterior cingulate gyrus, right and left lateral temporal lobe, and right and left superior parietal lobule.

Statistical Analysis

Descriptive characteristics are provided using averages, standard deviations, and percentiles. Examples of positive and negative scans are provided. Reader agreement was reported using the Kappa statistic (κ), and overall levels of agreement were also reported. Unilateral regional Z-scores and differences between amyloid-positive and amyloid-negative scans were reported. The area under the receiver-operating curve (AUC) was reported as a measure of overall predictive power for semi-quantitative Z-scores to identify amyloid-positive individuals. Regional spread of amyloid was reported using a number of regions exceeding 2.575 and 3.3 standard deviations above normal ($p = 0.01$ and $p = 0.001$, respectively). Patients were presented in rank order from the highest to the lowest mean amyloid positivity scores across unilateral regions (organized sequentially with left on top and right below). A two-tailed $\alpha = 0.05$ was used to determine statistical significance.

Results

A total of 167 subjects (83 females, 84 males; mean age 76.1 ± 6.8 years) underwent ^{18}F-florbetaben PET/CT. Of these cases, 92/167 (reader 1) and 101/167 scans (reader 2) scans were considered positive for amyloid deposition (agreement = 92.2%, κ = 0.84). ►**Figs. 1** and **2** demonstrate an example of a positive and negative amyloid brain PET, respectively, upon visual analysis. Notably, 12 of the 13 cases with visually discordant results were deemed positive in some or all regions by semiquantitative analysis. Upon repeat (unblinded) visual assessment, the readers sided with semiquantitative results in all but one case (92%). Furthermore, 4 of these 13 cases (31%) demonstrated advanced atrophy on structural imaging, which oftentimes poses a diagnostic challenge, especially for qualitative analysis.

An additional nine scans were subsequently identified as possible amyloid-positive based solely on semiquantitative analyses. The largest semiquantitative differences were identified in the left frontal lobe (Z = 7.74 in Aβ+ vs. 0.50 in Aβ− subjects), as depicted in ►**Table 1**. All unilateral regions showed statistically significant differences in Aβ burden ($p \leq 2.08E\text{-}28$ in all cases). Semiquantitative scores were highly sensitive to Aβ+ status and highly accurate in their ability to identify amyloid-positive patients (►**Table 2**), defined as a positive scan by both readers (AUC ≥ 0.90 [0.79–1.00]). Of the nine cases in which both reviewers evaluated the case to be negative and semiquantitative analysis deemed the case positive, advanced atrophy was present in three cases (33%). In addition, limited regional-only amyloid deposition was present in five of the nine cases (55%), which were positive solely by semiquantitative analysis.

Spread analyses suggested that amyloid deposition was most severe in the left posterior cingulate gyrus, where amyloid-positive individuals were most likely to cross standard cutoffs (►**Fig. 3**). Using a single Z-score cutoff as shown
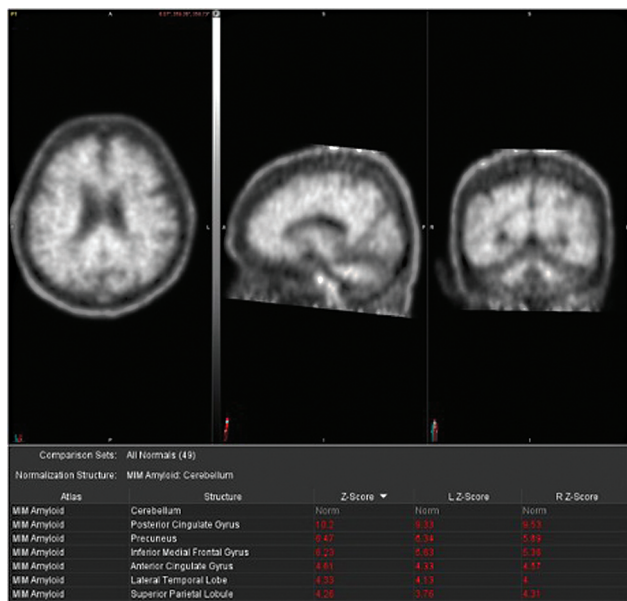
Fig. 1 (A) Positive ^{18}F-florbetaben PET/CT with diffuse tracer uptake in the cerebral cortex. (B) Semiquantitative analysis using the z-scores calculated in comparison to age-matched normal controls reveals significantly increased z-score values in analyzed brain regions including in the posterior cingulate gyrus, precuneus, inferior medial frontal gyrus, anterior cingulate gyrus, lateral temporal lobe, and superior parietal lobule (reference region: cerebellum).
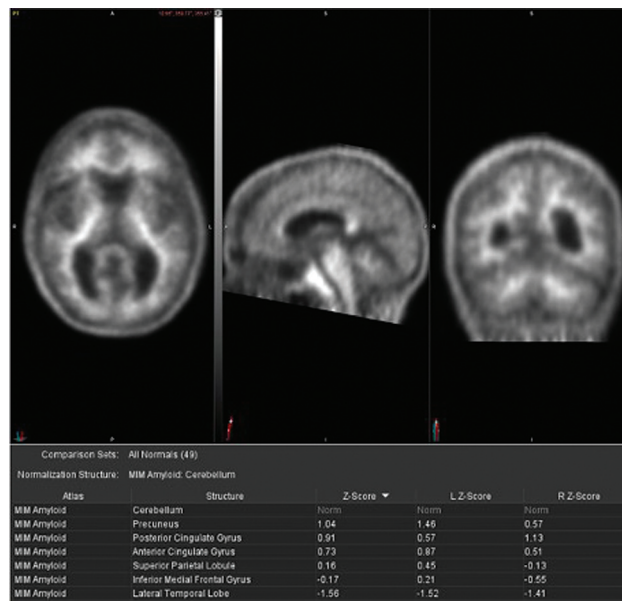
Fig. 2 (A) Negative ^{18}F-florbetaben PET/CT with tracer uptake only in the cerebral white matter, and no evidence of amyloid burden in the cerebral cortex. (B) Semiquantitative analysis using the z-scores calculated in comparison to age-matched normal controls reveals no significantly increased z-score values in analyzed brain regions including in the posterior cingulate gyrus, precuneus, inferior medial frontal gyrus, anterior cingulate gyrus, lateral temporal lobe, and superior parietal lobule (reference region: cerebellum).

Table 1 Regional Z-score differences between individuals determined to be visually positive versus negative on qualitative analysis

Region	Mean Z-score negative	SD negative	Mean Z-score positive	SD positive	Diff.	Area under the receiver-operating curve (95% C.I.)	*p*-Value
Left PCG	1.81	2.53	8.17	2.29	6.36	0.96 (0.93–1.00)	2.42E-35
Right PCG	1.99	2.51	8.09	2.31	6.11	0.96 (0.93–0.99)	7.16E-34
Left precuneus	1.07	2.07	8.22	2.43	7.15	0.98 (0.95–1.00)	1.10E-46
Right precuneus	1.09	1.93	7.18	2.17	6.09	0.97 (0.95–1.00)	3.73E-43
Left frontal	0.50	2.29	7.74	2.68	7.25	0.98 (0.95–1.00)	1.54E-42
Right frontal	0.36	2.36	7.03	2.48	6.67	0.97 (0.94–1.00)	5.34E-39
Left parietal	0.86	1.52	5.36	1.96	4.50	0.96 (0.94–0.99)	3.17E-37
Right parietal	0.79	1.35	4.33	1.62	3.54	0.94 (0.91–0.98)	2.17E-33
Left temporal	0.25	1.54	5.52	2.20	5.27	0.98 (0.96–1.00)	2.14E-41
Right temporal	0.37	1.41	4.86	2.10	4.50	0.96 (0.93–0.99)	1.01E-36
Left ACG	−0.08	2.00	4.34	2.05	4.42	0.94 (0.91–0.98)	4.38E-29
Right ACG	−0.13	2.09	4.40	2.13	4.53	0.90 (0.79–1.00)	2.08E-28

Abbreviations: ACG: anterior cingulate gyrus; AUC: area under the receiver-operating curve; Diff.: difference between amyloid+ and amyloid-participants; PCG: posterior cingulate gyrus; 95% CI: 95% confidence interval.

in ►**Fig. 3A**, the largest differences between negative and positive individuals were in the left frontal lobe, and analyses using region-specific cutoffs indicated that the presence of amyloid in the temporal and anterior cingulate cortex, while exhibiting relatively low Z-scores, was the most common. Of note, among individuals whose qualitative and quantitative results were non-concordant, quantitative measures of am-yloid positivity were the lowest in the temporal and parietal lobes potentially suggesting that qualitative examinations are more difficult in these regions. By examining spread using the region-specific cutoffs determined in this study as shown in ►**Fig. 3B**, we found that though having relatively low Z-scores, amyloid was more often elevated in the temporal lobe and anterior cingulate gyri. Of note, when the

Table 2 Cut points derived for each cortical region along with sensitivity and specificity at the optimal cut point

Regional Z-scores	Suggested cutoffs	Sensitivity at cutoff	Specificity at cutoff
Left PCG	4.63	0.94	0.93
Right PCG	5.38	0.90	0.94
Left precuneus	3.87	0.97	0.96
Right precuneus	4.58	0.90	0.96
Left frontal	3.82	0.96	0.96
Right frontal	3.24	0.96	0.94
Left parietal	3.20	0.85	0.96
Right parietal	1.69	0.94	0.82
Left temporal	2.21	0.95	0.93
Right temporal	2.09	0.95	0.90
Left ACG	1.65	0.90	0.87
Right ACG	1.44	0.94	0.83

Abbreviations: ACG: anterior cingulate gyrus; PCG: posterior cingulate gyrus.

temporal lobe and anterior cingulate gyrus were elevated, but other regions including the frontal and posterior cingulate gyrus were not sufficient to cross relatively higher Z-score cutoffs in those regions, qualitative results were often discordant from the quantitative results.

Discussion

Amyloid PET provides a critical clinical neuroimaging tool in patients with possible AD. The purpose of this study was to evaluate whether qualitative adjudication of Aβ positivity in the clinical setting may be facilitated by relying on results from semi-quantitative Z-score analysis.

Amyloid PET allows for in vivo visualization of β-amyloid deposition, a hallmark pathologic change in AD that has been described to be the earliest neuroimaging predictor of future cognitive impairment in healthy elderly.[21] Available amyloid-targeting PET radiotracers include the research radiotracer [^{11}C]-Pittsburgh compound (PiB), as well as three FDA-approved [^{18}F]-labeled radiopharmaceuticals (florbetaben, florbetapir, and flutemetamol), all of which demonstrate high-affinity binding to cortical β-amyloid plaques.[22,23] While most of the early studies used [^{11}C]-PiB, the short half-life of ^{11}C limits its pragmatic clinical use. All three FDA-approved amyloid radiotracers have been shown to be acceptable clinical surrogates for PiB in the detection of Aβ and are widely used, with reported sensitivity and specificity of 90% or higher for the detection of increased cortical amyloid burden. In one study, cortical retention for each pair of tracers was strongly correlated, regardless of reference region (PiB-flutemetamol, $\rho = 0.84$–0.99; PiB-florbetapir, $\rho = 0.83$–0.97) and analysis method ($\rho = 0.90$–0.99).[24,25] Similarly, there was a strong association between PiB and florbetapir cortical retention ratios (Spearman $\rho = 0.86$–0.95). In another study, there was an excellent linear

correlation between PiB and florbetaben global SUVR values ($r = 0.97$, $p < 0.0001$) with similar effect sizes for distinguishing AD from control subjects for both radiotracers (Cohen's $d = 3.3$ for PiB and 3.0 for florbetaben).[26]

Clinical interpretation is typically binary: "amyloid-positive" when there is evidence of cortical uptake and loss of gray–white matter differentiation versus "amyloid-negative" when there is non-specific white matter uptake and lack of cortical uptake resulting in preserved gray–white matter differentiation (►**Figs. 1** and **2**).[27] While amyloid PET can reliably detect β-amyloid deposition in vivo, the amyloid burden does not correlate with the degree of cognitive impairment,[21] and β-amyloid deposition can be seen in healthy older adults, adding an additional dimension to image interpretation in the clinical setting.[28,29] Therefore, a positive amyloid PET scan is necessary but insufficient to provide a positive diagnosis of AD, though a negative amyloid uptake has a good negative predictive value for AD. Among Medicare beneficiaries with MCI or dementia of uncertain etiology evaluated by specialists as part of the ACR-sponsored IDEAS study, amyloid PET was associated with changes in clinical management in over 60% of cases, while the etiologic diagnosis changed from AD to non-AD and vice versa in 35% of patients.[30] Furthermore, Aβ-amyloid PET imaging is widely used in patient selection and evaluation of treatment response and target engagement in disease-modifying clinical trials, and is expected to become a staple in the clinical management of AD patients, given recent regulatory approval of aducanumab, a high-affinity, fully human IgG1 monoclonal antibody against a conformational epitope found on Aβ in the brain.[14]

Quantitative PET measurements have been reported to have a good correlation with visual interpretations, and standardized uptake value ratio (SUVR) and regional counts per reference count have been commonly used in quantitative analysis of amyloid PET.[31] Prior studies in the literature have assessed kinetic model-based approaches to quantify β-amyloid binding in the brain from dynamic PET data. For example, Becker et al[15] performed ^{18}F-florbetaben PET with concurrent multiple arterial sampling after tracer injection in AD subjects and controls. Regional brain-tissue time-activity curves for 90 min were analyzed by a one-tissue-compartment model and a two-tissue-compartment model (2TCM) with metabolite-corrected plasma data estimating the specific distribution volume (VS) and distribution volume ratio (DVR [2TCM]) and a multilinear reference tissue model estimating DVR (DVR [MRTM]) using the cerebellar cortex as the reference tissue. In their study, all β-amyloid-binding parameters (VS, DVR [2TCM], DVR [MRTM], and SUVR) were significantly increased in AD patients and excellent in discriminating between β-amyloid-positive and -negative scans. Furthermore, most amyloid PET cases can be easily classified as positive or negative on the bases of visual assessment; however, the findings are equivocal in approximately 10% of cases.[32] Because conventional mean cortical SUVR measures accumulation in both gray matter (GM) and white matter, it may misestimate amyloid deposits. Therefore, Ishii et al[16] developed a regional gray matter-dedicated
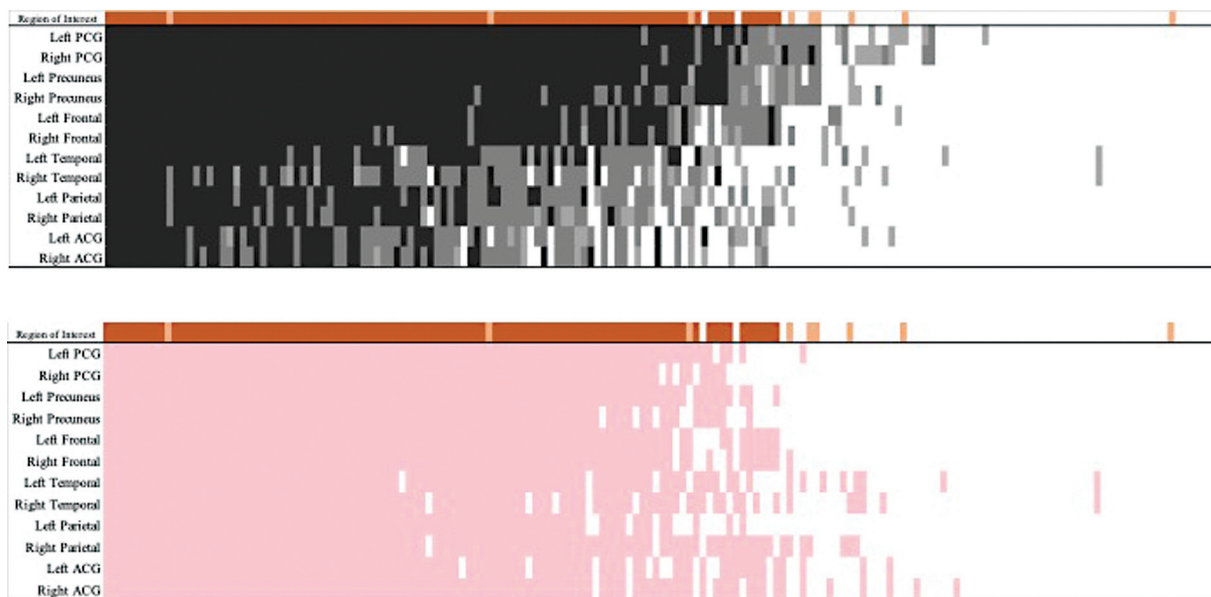
Fig. 3 Regional amyloid positivity analysis across patients. Patients are presented in rank order from the highest to the lowest mean amyloid positivity scores across unilateral regions (organized sequentially with left on top and right below). Regions are ordered from most affected (*top*) to least affected. Qualitative analysis status is shown using orange bars along the top, with two positive reads indicated by the presence of a dark orange bar and a single positive read indicated by a lighter orange bar. Panel A: Person-region observations are colored based on deviation from expectations (2.58 SDs are light gray, 3.3 SDs are dark gray, 5 SDs are charcoal). Panel B: Person-region observations are colored based on whether that observation cleared the estimated region-specific cutoffs noted in ►**Table 2**. ACG: anterior cingulate gyrus; PCG: posterior cingulate gyrus. Amyloid positivity status was determined qualitatively and shown using dark orange if both visual readers identified the person as positive, and light orange if only one reader identified the visual positive.

SUVR (GMSUVR) system for amyloid PET images with three-dimensional (3D-MRI) and demonstrated its utility for discriminating between amyloid-positive and -negative subjects, even in cases where qualitatively, amyloid deposition was equivocal. In addition, neocortical atrophy typically present in elderly patients also reduces PET signal intensity, potentially affecting the diagnostic efficacy of β-amyloid PET data. Rullman et al[33] used partial-volume effect correction (PVEC), to adjust for atrophy bias, and demonstrated that PVEC improves quantitative analysis of ^{18}F-florbetaben PET scans. In clinical practice, careful attention should be paid to the selection of regions of interest (ROIs) by post-processing software as it may be suboptimal, particularly in small and adjacent regions such as the cingulate cortices, and in cases of advanced atrophy on structural imaging.[34,35] More recently, the Centiloid Project working group standardized quantitative amyloid imaging measures by scaling the outcome of each particular analysis method or tracer to a 0 to 100 scale, anchored by young controls ($\leq$ 45 years) and typical AD patients, with units of this scale referred to as "Centiloids" for PiB PET and all three ^{18}F-labelled FDA-approved amyloid PET tracers.[36,37]

Heavily quantitative approaches are cumbersome, require a trained quantitative analyst, and may not be feasible in a busy clinical practice. Additionally, not all clinical centers have access to the high-resolution 3D MRI sequences needed to help with this process. In a clinical setting, qualitative adjudication of Aβ positivity in clinical amyloid PET studies may be facilitated by relying on results from semi-quantitative Z-score

analysis, which is of practical benefit, especially to trainees and inexperienced or infrequent readers. Therefore, we evaluated the correspondence between visual assessment and semiquantitative analysis in evaluating the cortical amyloid burden on clinical amyloid PET scans. Limitations of this study include its retrospective nature and lack of longitudinal follow-up. Additionally, only a single vendor post-processing algorithm was validated. Replication of these findings on other clinical PET software tools is needed prior to widespread implementation in routine clinical practice.

In conclusion, visual assessment and semiquantitative z-score analysis provide highly congruent results, thereby enhancing reader confidence and improving scan interpretation. This is particularly relevant given the recent emphasis on amyloid-targeting disease-modifying therapeutics, as they emerge from the research setting and enter clinical practice.

References

1 Arvanitakis Z, Shah RC, Bennett DA. Diagnosis and management of dementia: review. JAMA 2019;322(16):1589–1599. Doi: 10.1001/jama.2019.4782
2 2021 Alzheimer's disease facts and figures. Alzheimers Dement 2021;17(03):327–406. Doi: 10.1002/alz.12328

3 Hebert LE, Weuve J, Scherr PA, Evans DA. Alzheimer disease in the United States (2010-2050) estimated using the 2010 census. Neurology 2013;80(19):1778–1783

4 Alzheimer A. Ueber eine eigenartige erkrankung der hirnrinde. Z Gesamte Neurol Psychiatr 1907;18:177–179

5 Perl DP. Neuropathology of Alzheimer's disease. Mt Sinai J Med 2010;77(01):32–42. Doi: 10.1002/msj.20157

6 Serrano-Pozo A, Frosch MP, Masliah E, Hyman BT. Neuropathological alterations in Alzheimer disease. Cold Spring Harb Perspect Med 2011;1(01):a006189. Doi: 10.1101/cshperspect.a006189

7 Thal DR, Rüb U, Orantes M, Braak H. Phases of a beta-deposition in the human brain and its relevance for the development of AD. Neurology 2002;58(12):1791–1800. Doi: 10.1212/wnl.58.12.1791

8 Hanseeuw BJ, Betensky RA, Jacobs HIL, et al. Association of amyloid and tau with cognition in preclinical Alzheimer disease: a longitudinal study. JAMA Neurol 2019;76(08):915–924. Doi: 10.1001/jamaneurol.2019.1424 Erratum in: JAMA Neurol. 2019 Aug 1;76(8):986. PMID: 31157827; PMCID: PMC6547132

9 Cho H, Lee HS, Choi JY, et al. Predicted sequence of cortical tau and amyloid-β deposition in Alzheimer disease spectrum. Neurobiol Aging 2018;68:76–84. Doi: 10.1016/j.neurobiolaging.2018.04.007

10 Cummings J, Lee G, Ritter A, Sabbagh M, Zhong K. Alzheimer's disease drug development pipeline: 2020. Alzheimers Dement (N Y) 2020;6(01):e12050. Doi: 10.1002/trc2.12050. PMID: 32695874; PMCID: PMC7364858

11 Jack CR Jr, Bennett DA, Blennow K, et al. A/T/N: an unbiased descriptive classification scheme for Alzheimer disease biomarkers. Neurology 2016;87(05):539–547. Doi: 10.1212/WNL.0000000000002923

12 Jack CR Jr, Bennett DA, Blennow K, et al; Contributors. NIA-AA research framework: toward a biological definition of Alzheimer's disease. Alzheimers Dement 2018;14(04):535–562

13 Knopman DS, Haeberlein SB, Carrillo MC, et al. The National Institute on Aging and the Alzheimer's Association Research Framework for Alzheimer's disease: perspectives from the research roundtable. Alzheimers Dement 2018;14(04):563–575. Doi: 10.1016/j.jalz.2018.03.002

14 FDA Grants Accelerated Approval for Alzheimer's Drug Accessed: July 25, 2021, at: https://www.fda.gov/news-events/press-announcements/fda-grants-accelerated-approval-alzheimers-drug

15 Becker GA, Ichise M, Barthel H, et al. PET quantification of 18F-florbetaben binding to β-amyloid deposits in human brains. J Nucl Med 2013;54(05):723–731

16 Ishii K, Yamada T, Hanaoka K, et al. Regional gray matter-dedicated SUVR with 3D-MRI detects positive amyloid deposits in equivocal amyloid PET images. Ann Nucl Med 2020;34(11):856–863. Doi: 10.1007/s12149-020-01513-3

17 Akamatsu G, Ikari Y, Ohnishi A, et al; Japanese Alzheimer's Disease Neuroimaging Initiative. Voxel-based statistical analysis and quantification of amyloid PET in the Japanese Alzheimer's disease neuroimaging initiative (J-ADNI) multi-center study. EJNMMI Res 2019;9(01):91. Doi: 10.1186/s13550-019-0561-2

18 Imaging Dementia-Evidence for Amyloid Scanning (IDEAS) Study. Accessed July 25, 2021, at: https://clinicaltrials.gov/ct2/show/NCT02420756

19 Johnson KA, Minoshima S, Bohnen NI, et al. Appropriate use criteria for amyloid PET: a report of the Amyloid Imaging Taskforce, the Society of Nuclear Medicine and Molecular Imaging, and the Alzheimer's Association. Alzheimers Dement 2013;9(01):e-1–e-16. Doi: 10.1016/j.jalz.2013.01.002

20 Minoshima S, Drzezga AE, Barthel H, et al. SNMMI procedure standard/EANM practice guideline for amyloid PET imaging of the brain 1.0. J Nucl Med 2016;57(08):1316–1322. Doi: 10.2967/jnumed.116.174615

21 Murray ME, Lowe VJ, Graff-Radford NR, et al. Clinicopathologic and 11C-Pittsburgh compound B implications of Thal amyloid phase across the Alzheimer's disease spectrum. Brain 2015;138 (Pt 5):1370–1381. Doi: 10.1093/brain/awv050

22 Nasrallah IM, Wolk DA. Multimodality imaging of Alzheimer disease and other neurodegenerative dementias. J Nucl Med 2014;55(12):2003–2011. Doi: 10.2967/jnumed.114.141416

23 Villemagne VL, Barkhof F, Garibotto V, Landau SM, Nordberg A, van Berckel BNM. Molecular Imaging Approaches in Dementia. Radiology 2021;298(03):517–530. Doi: 10.1148/radiol.2020200028

24 Landau SM, Thomas BA, Thurfjell L, et al; Alzheimer's Disease Neuroimaging Initiative. Amyloid PET imaging in Alzheimer's disease: a comparison of three radiotracers. Eur J Nucl Med Mol Imaging 2014;41(07):1398–1407. Doi: 10.1007/s00259-014-2753-3

25 Landau SM, Breault C, Joshi AD, et al; Alzheimer's Disease Neuroimaging Initiative. Amyloid-β imaging with Pittsburgh compound B and florbetapir: comparing radiotracers and quantification methods. J Nucl Med 2013;54(01):70–77. Doi: 10.2967/jnumed.112.109009

26 Villemagne VL, Mulligan RS, Pejoska S, et al. Comparison of 11C-PiB and 18F-florbetaben for Aβ imaging in ageing and Alzheimer's disease. Eur J Nucl Med Mol Imaging 2012;39(06):983–989. Doi: 10.1007/s00259-012-2088-x

27 Lundeen TF, Seibyl JP, Covington MF, Eshghi N, Kuo PH. Signs and artifacts in amyloid PET. Radiographics 2018;38(07):2123–2133

28 Clark CM, Schneider JA, Bedell BJ, et al; AV45-A07 Study Group. Use of florbetapir-PET for imaging beta-amyloid pathology. JAMA 2011;305(03):275–283

29 Barthel H, Luthardt J, Becker G, et al. Individualized quantification of brain β-amyloid burden: results of a proof of mechanism phase 0 florbetaben PET trial in patients with Alzheimer's disease and healthy controls. Eur J Nucl Med Mol Imaging 2011;38(09):1702–1714. Doi: 10.1007/s00259-011-1821-1

30 Rabinovici GD, Gatsonis C, Apgar C, et al. Association of amyloid positron emission tomography with subsequent change in clinical management among Medicare beneficiaries with mild cognitive impairment or dementia. JAMA 2019;321(13):1286–1294. Doi: 10.1001/jama.2019.2000

31 Yamane T, Ishii K, Sakata M, et al; J-ADNI Study Group. Inter-rater variability of visual interpretation and comparison with quantitative evaluation of 11C-PiB PET amyloid images of the Japanese Alzheimer's Disease Neuroimaging Initiative (J-ADNI) multicenter study. Eur J Nucl Med Mol Imaging 2017;44(05):850–857. Doi: 10.1007/s00259-016-3591-2

32 Hosokawa C, Ishii K, Hyodo T, et al. Investigation of (11)C-PiB equivocal PET findings. Ann Nucl Med 2015;29(02):164–169. Doi: 10.1007/s12149-014-0924-8

33 Rullmann M, Dukart J, Hoffmann KT, et al. Partial-volume effect correction improves quantitative analysis of 18F-florbetaben β-amyloid PET scans. J Nucl Med 2016;57(02):198–203. Doi: 10.2967/jnumed.115.161893

34 Sarikaya I, Kamel WA, Ateyah KK, Essa NB, AlTailji S, Sarikaya A. Visual versus semiquantitative analysis of 18F- fluorodeoxyglucose-positron emission tomography brain images in patients with dementia. World J Nucl Med 2021;20(01):82–89. Doi: 10.4103/wjnm.WJNM_53_18

35 Sarikaya I, Sarikaya A, Elgazzar AH. Current status of 18F-FDG PET brain imaging in patients with dementia. J Nucl Med Technol 2018;46(04):362–367. Doi: 10.2967/jnmt.118.210237

36 Klunk WE, Koeppe RA, Price JC, et al. The Centiloid Project: standardizing quantitative amyloid plaque estimation by PET. Alzheimers Dement 2015;11(01):1–15.e1, 4. Doi: 10.1016/j.jalz.2014.07.003

37 Rowe CC, Doré V, Jones G, et al. 18F-Florbetaben PET beta-amyloid binding expressed in Centiloids. Eur J Nucl Med Mol Imaging 2017;44(12):2053–2059. Doi: 10.1007/s00259-017-3749-6